

# FAST NONLINEAR SEISMIC SSI ANALYSIS USING A HYBRID TIME-COMPLEX FREQUENCY APPROACH FOR LOW-RISE NUCLEAR CONCRETE SHEARWALL BUILDINGS

Dan M. Ghiocel <sup>1</sup>

<sup>1</sup> Chief of Engineering, Ghiocel Predictive Technologies, Inc., New York, USA

## ABSTRACT

The paper presents a highly efficient nonlinear SSI approach based on a hybrid time-complex frequency approach using an iterative procedure. The hybrid approach uses a piece-wise equivalent-linearization for computing the FEA solution in complex frequency. The local linearized hysteretic models are calibrated based on the “true” nonlinear concrete wall behaviour in time domain. Sophisticated shear deformation hysteretic models with pinching were implemented. Comparative results of the hybrid approach and the *true* nonlinear time-integration approach showed very good matching. The hybrid approach is applicable to nonlinear SSI analysis for i) *design level* for correctly including the concrete cracking in structures as a function of stress levels in accordance to the new ASCE 04-2015 standard (Sections 3.2.2 and 3.3.2) and the USNRC SRP requirements, and ii) *beyond design level* in accordance with the ASCE 43-2005 recommendations, to properly compute the inelastic absorption factors for structural fragility analyses. The paper presents a validation case study of a typical low-rise shearwall nuclear structure for which the hybrid approach results are compared with the “true” nonlinear time-integration approach results. Nonlinear SSI analyses performed for rigid rock and soft soil sites demonstrate the capabilities of the hybrid approach. The nonlinear SSI hybrid approach is also much faster and robust than the “true” nonlinear SSI time-integration approach.

## INTRODUCTION

The fast nonlinear SSI approach uses an iterative equivalent linear procedure in complex frequency domain to solve repeatedly the linearized SSI system FEA solution. The nonlinear concrete hysteretic response is computed using wall *panels* defined as “macro shell elements”. For each shearwall *panel*, the hysteretic shear force is computed in time domain using the nodal panel SSI displacements. The nodal displacements are applied as boundary conditions to the nonlinear concrete wall panels. The iterative approach is fast convergent in only few iterations.

For typical nuclear applications, the nonlinear SSI analysis in complex frequency via the proposed hybrid approach is tens to hundreds times faster than the nonlinear SSI analysis in time domain. In addition to the computational speed aspect, the complex frequency nonlinear SSI approach via local equivalent linearization is much simpler to apply and much more numerically robust than the time domain nonlinear SSI approaches that need very small integration time steps to avoid noisy results, as also recognized by many researchers including the MIT researchers (Kausel and Assimaki, 2002).

The engineering literature includes various hysteretic models for the idealization of the reinforced concrete shearwall behaviour. For the low-rise shearwall buildings that are of interest for nuclear buildings, from various hysteretic models, we selected the Cheng-Mertz hysteretic model (Cheng and Mertz, 1989) that was used over years in a number of studies for the DOE and ASCE standards.

Figure 1 shows the Cheng-Mertz hysteretic models for the shear and bending behaviour in the low-rise shearwalls. The figure includes a comparison between experimental testing and numerical simulation

using Cheng-Mertz hysteretic of a shearwall panel (Chen and Mertz, 1989). Figure 2 shows a comparison of the Chen-Mertz models for Shear (CMS) and Bending (CMB) against the popular Takeda model for a shearwall panel assuming that all models have the same backbone curve and displacement history inputs. Figure 2 shows the hysteretic loop response comparisons for two material backbone (BBC) curves with different concrete cracking thresholds. The cracking threshold point is plotted on BBC with a black dot. Thus, for low cracking thresholds the CMS hysteretic loops are pinched, while the CMB and Takeda loops are not. Thus, for BBC with low cracking thresholds for which pinching occurs, the CMB and Takeda models may dissipate more energy than CMS that is capable of capturing well pinching effects.

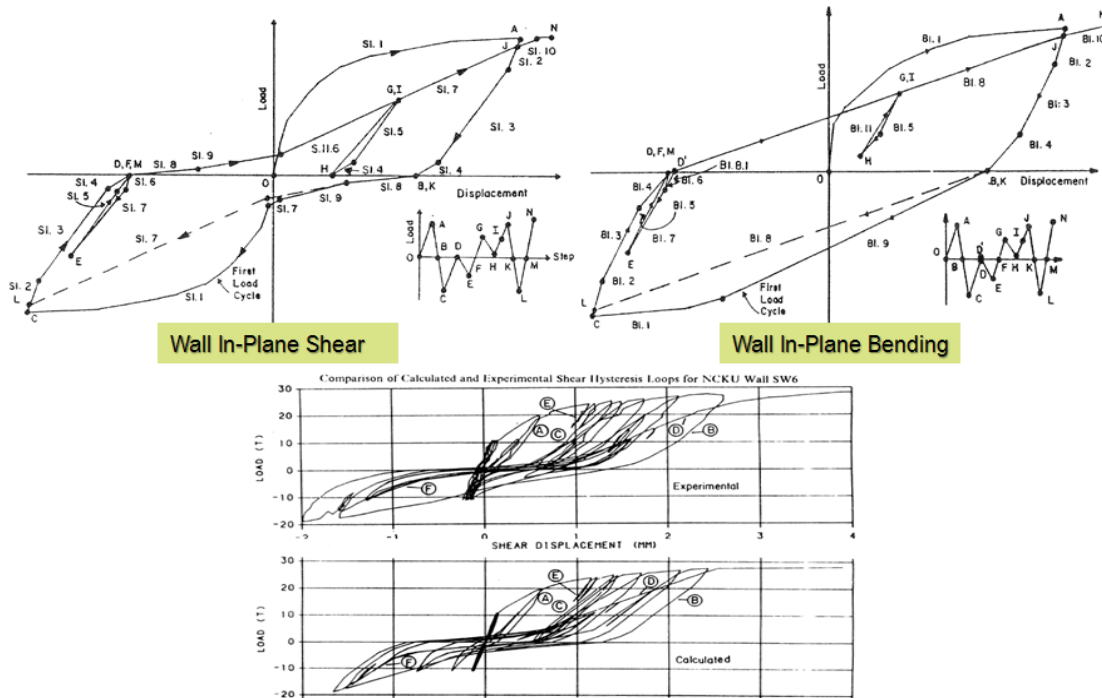


Figure 1 Chen-Mertz Hysteretic Models for Shear Deformation (CMS) and Bending Deformation (CMB)

The nonlinear SSI analysis hybrid approach as implemented in the ACS SASSI Option NON software (2015) includes the following computational steps:

- 1) For the initial iteration, perform the linear SSI analysis using the elastic material stiffness and damping properties for all shearwall panels
- 2) Compute the concrete shearwall panel shear force responses in time domain that are further used to calibrate the local panel linearized hysteretic models in complex frequency
- 3) Perform a new SSI analysis iteration using reanalysis (restart analysis) in the complex frequency domain using the hysteretic models computed in Step 2 for all selected panels
- 4) Check convergence of the nonlinear SSI response after new SSI iteration, and go back to Step 2 if convergence is not achieved. Otherwise continue with a new iteration going back to Step 2.

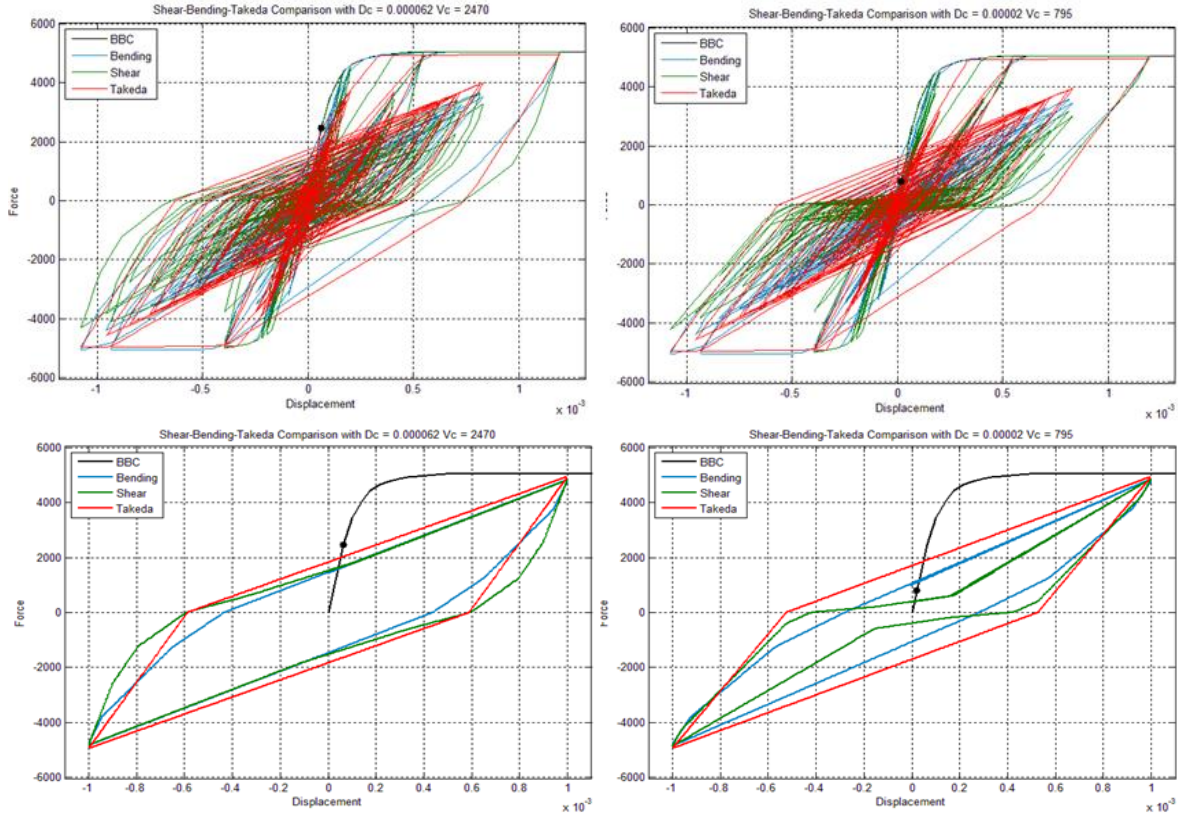


Figure 2 Comparison of CMS, CMB and Takeda Hysteretic Model Responses for Same Inputs

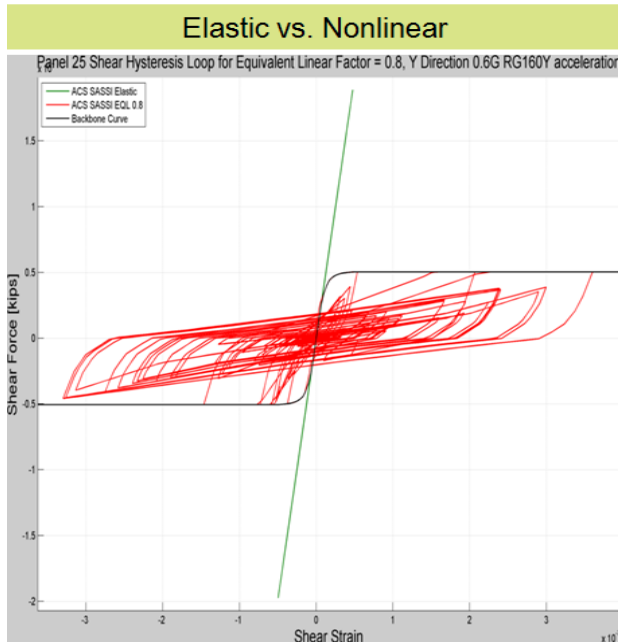


Figure 3 Linear versus Nonlinear Behavior

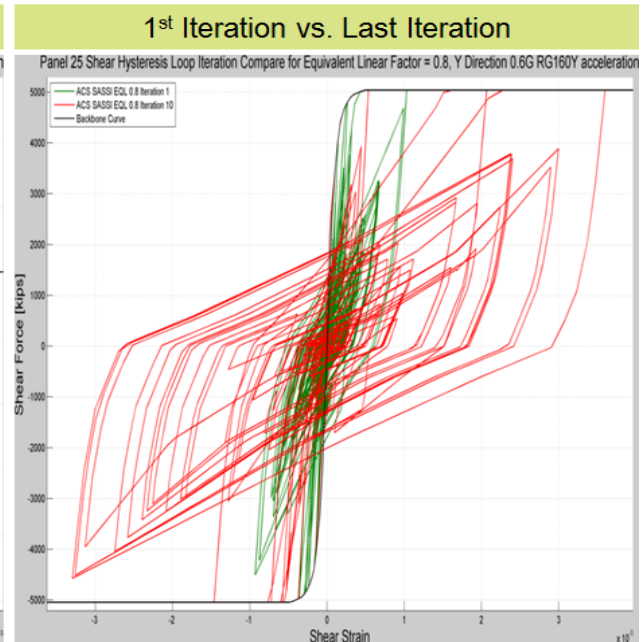


Figure 4 1<sup>st</sup> versus Last Nonlinear Iteration

A typical nonlinear SSI analysis result using the hybrid approach is shown in Figure 3 (for Panel 25 in Figure 6). The plots in Figure 3 show a comparison of a concrete shearwall panel hysteretic behavior

computed for the linear elastic structure in the first SSI iteration and in the nonlinear structure in the last SSI iteration, for a beyond-design earthquake that is twice than the design earthquake. The green line shows the linear elastic shear force-displacement variation, while the red line shows the nonlinear shear force-displacement variation in the last iteration. The computed inelastic response of the concrete wall panel appears to be close to structure collapse. The computed ductility factors with respect to yielding appears to be about 8-10 (since no clear yielding point defined in BBC), the maximum normalized story drifts (shear strain) about 0.004 and the computed inelastic absorption reduction factor about 3.50.

Figure 4 shows a comparison between the nonlinear hysteretic loops computed after the 1<sup>st</sup> SSI iteration and after the last iteration for the same panel for the beyond-design earthquake. The 1<sup>st</sup> SSI iteration results are far from the converged results. Additional 5 SSI iterations (SSI reanalyses) were required for the nonlinear result convergence. *These results alert against published papers that recommend for nonlinear SSI analysis the use of a cascaded SSI approach with no SSI iterations.*

## VALIDATION CASE STUDY

A case study of a typical low-rise shearwall nuclear plant structure (Figure 5) is shown to demonstrate the application of the nonlinear SSI approach in complex frequency. The nonlinear hysteretic behaviour is determined based on the computed panel drifts and the shear forces, assuming a Cheng-Mertz shear (CMS) deformation model. The computed story drifts exclude the panel rigid body rotations coming from the SSI rocking modes that do not produce any stresses in the panel.

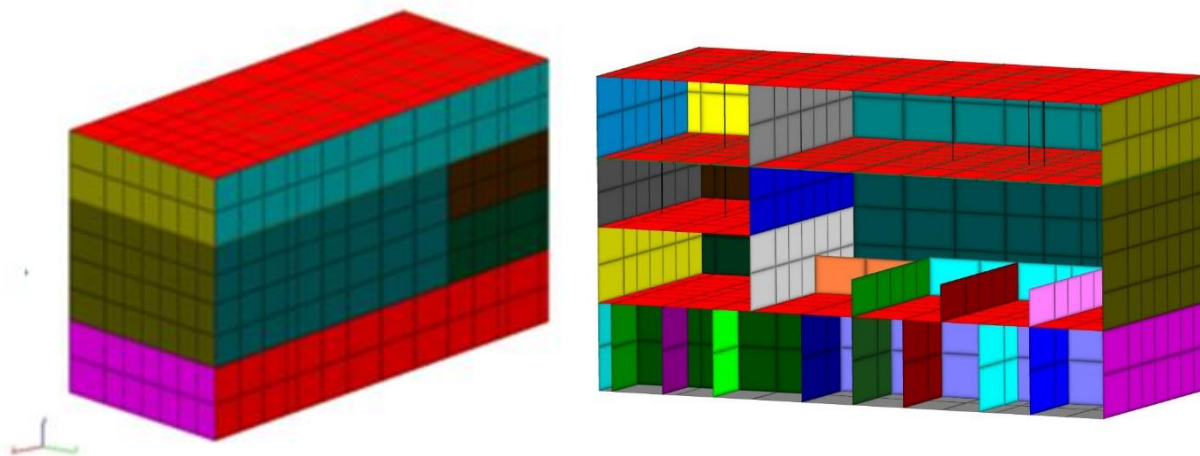


Figure 5 Low-Rise Concrete Shearwall Building; Outside View (left) and Section View (right)

The first step in the nonlinear SSI analysis as implemented in ACS SASSI is to create the concrete wall panels (macro shell elements) with nonlinear behaviour. Using the SUBMODELER GUI module specialized commands, such as *Wallfr*, *Panelize*, *MergeGroup* and *SplitGroups*, the structural walls can be effectively partitioned per floors. The entire model preparation process is almost automatic, so that it takes only a couple of hours to finalize a complex nonlinear FEA model. Figures 5 and 6 show the split of the investigated shearwall structure in various nonlinear wall panels.

An aspect of key importance for the nonlinear analysis input are the constitutive force-displacement curves or the backbone curves (BBC) for each structural wall panel. In ACS SASSI, using the SUBMODELER module *BBC* command, the constitutive curves can be generated very rapidly. A key parameter of the BBC curves is the shear capacity value for the shearwall panel. Various options for computing shear capacity for flanged and non-flanged concrete walls were implemented in accordance

with the new ASCE 43-2015 draft recommendations are based on the experimental shearwall panel testing database at the University of New York at Buffalo (Gulec and Whittaker, 2009).

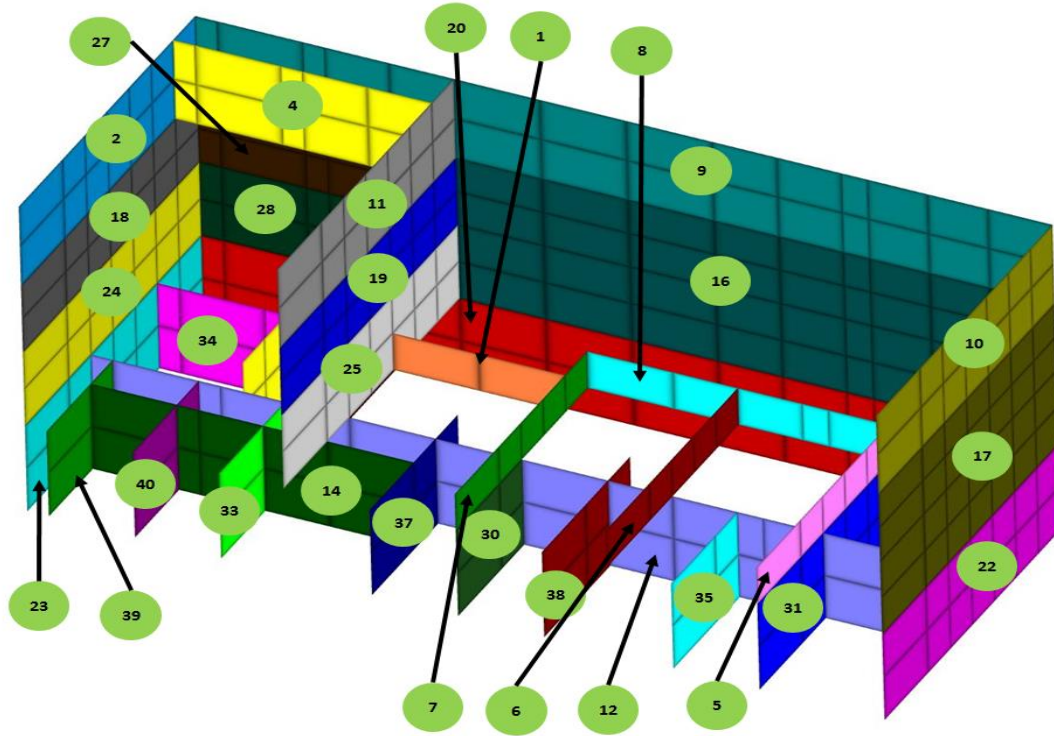


Figure 6 Shearwall Building View With 40 Wall Panels Used for Nonlinear Structure Analysis

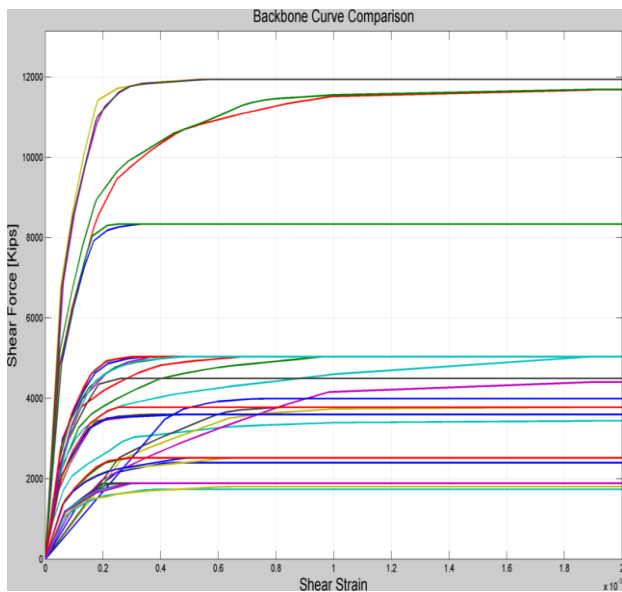


Figure 7 The BBC for Shearwall Panels

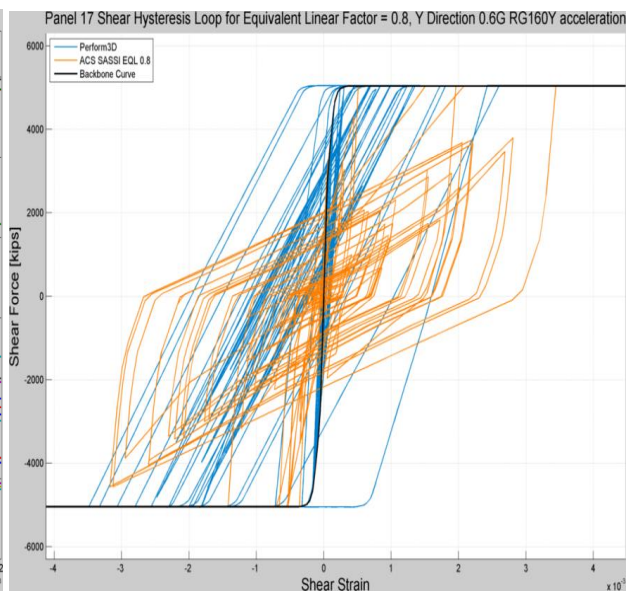


Figure 8 Comparison of Hysteretic Models

The hybrid approach, as implemented in ACS SASSI, was validated for the low-rise shearwall structure in Figures 5 and 6 against the “true” nonlinear time-history analysis, as implemented in the specialized PERFORM3D software (trademark of Computer Structures, Inc.). The two FEA computer codes were

applied to the *fixed-base* model of the low-rise shearwall structure for the same analysis inputs. Using PERFORM3D a nonlinear pushover analysis was performed to create the BBC for the entire structure and the BBC for each wall panel, as illustrated in Figure 7. The input acceleration time histories were simulated based on the RG 1.60 design spectrum anchored at 0.30g and 0.60g ZPGA. However, the shear force hysteretic models were different. For the ACS SASSI analysis we used the Cheng-Mertz (CMS) model, while for PERFORM3D analysis we selected the fiber model applicable to the low-rise shearwall panels. Figure 8 shows the two model hysteretic loops for the same story drift history. The Cheng-Mertz shear model (brown line in Figure 8) appears to be more refined since degrades the loading-unloading stiffness as a result of the concrete degradation, and also captures accurately the pinching effects characteristics to shear deformation models (origin oriented type). The fiber model (blue line in Figure 8) shows no stiffness degradation and low energy dissipation for the small amplitude cycles with no trace of pinching.

Comparisons between ACS SASSI results and PERFORM3D were done for both 0.30g and 0.60g ZPGA earthquake levels. The convergence of the iterative hybrid approach was achieved in 4-5 SSI iterations for 0.30g input and 6-7 SSI iterations for 0.60g input. This 5 to 7 number of iterations implies a nonlinear SSI analysis runtime of about 2-3 times of the linear elastic SSI analysis runtime, if the appropriate SSI analysis restart options are selected.

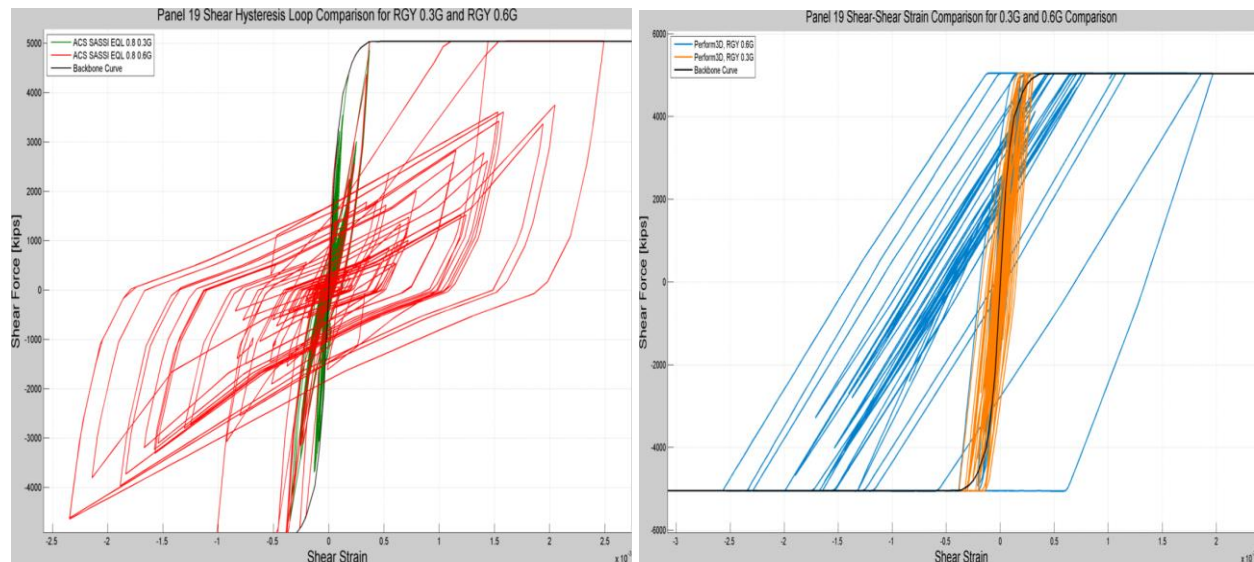


Figure 9 Panel 17 Hysteretic Loops Computed for 0.30g and 0.60g Using ACS SASSI Cheng-Mertz Model (left) After Final Iteration and PERFORM3D Fiber Model (right)

Figure 9 shows the hysteretic loops for Panel 17 (see Figure 6 for the panel location) using the two FEA codes for the 0.30g and 0.60g seismic inputs. The maximum absolute value of the normalized inelastic story drifts (shear strain) was 0.0025 for both the hybrid approach and true nonlinear time approach.

Figure 10 shows the deformation of the nonlinear structure computed using the two FEA codes for the fixed-base models, ACS SASSI (left) and PERFORM3D (right) at the same time moment, specifically at 7.285 seconds of the 0.60g earthquake duration. For a more detailed comparison that includes side-to-side structural animations for a part of the duration of the 0.60g earthquake input, see [http://www.ghiocel-tech.com/enggTools/ACS\\_SASSI\\_vs\\_Perform3D\\_Nonlinear\\_Response\\_for\\_Rigid\\_Foundation\\_0.6g\\_Acc.avi](http://www.ghiocel-tech.com/enggTools/ACS_SASSI_vs_Perform3D_Nonlinear_Response_for_Rigid_Foundation_0.6g_Acc.avi). These side-by-side animations illustrate a very good matching between the two FEA codes results.

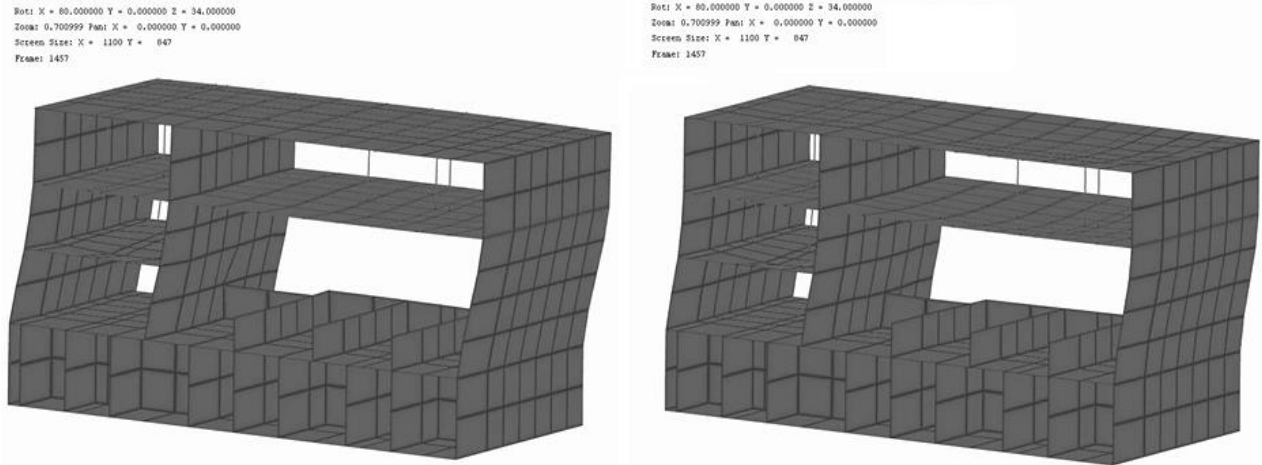


Figure 10 Structural Deformation Computed at the 7.285 Sec. Time for 0.60g Seismic Input for ACS SASSI Option NON (left) and PERFORM3D (right)

Figure 11 shows a comparison of the computed inelastic story drift histories in Panels 17 and 19 (see Figure 6 for their locations) for the 0.60g seismic input. The matching between the ACS SASSI iterative solution (red) and PERFORM3D nonlinear time history solution (green) is also very good. The SSI motion phasing is very well captured by the hybrid approach. The main difference between the two FEA solutions, is the shift to negative values that occurs for the time-domain solution that indicates a permanent story drift.



Figure 11 Story Drifts for Panels 17 and 19 Computed Using ACS SASSI Iterative Approach and PERFORM3D Time-Domain Integration Approach

The shear force inelastic reduction factors computed for each panel for the 0.30g and 0.60g earthquakes in the Y-direction (transverse) using ACS SASSI (colored line) and PERFORM3D (black line) are plotted in Figure 12. The iterative SSI runs were done for three effective strain reduction factor (SRF) values of 0.60, 0.80 and 1.0. The differences in results for the three SRF input values are negligible. The matching between the computed inelastic factors was very good. Please note that the X-direction (longitudinal) panels have zero inelastic factors (negligible shear forces) since seismic input is only in Y-direction.

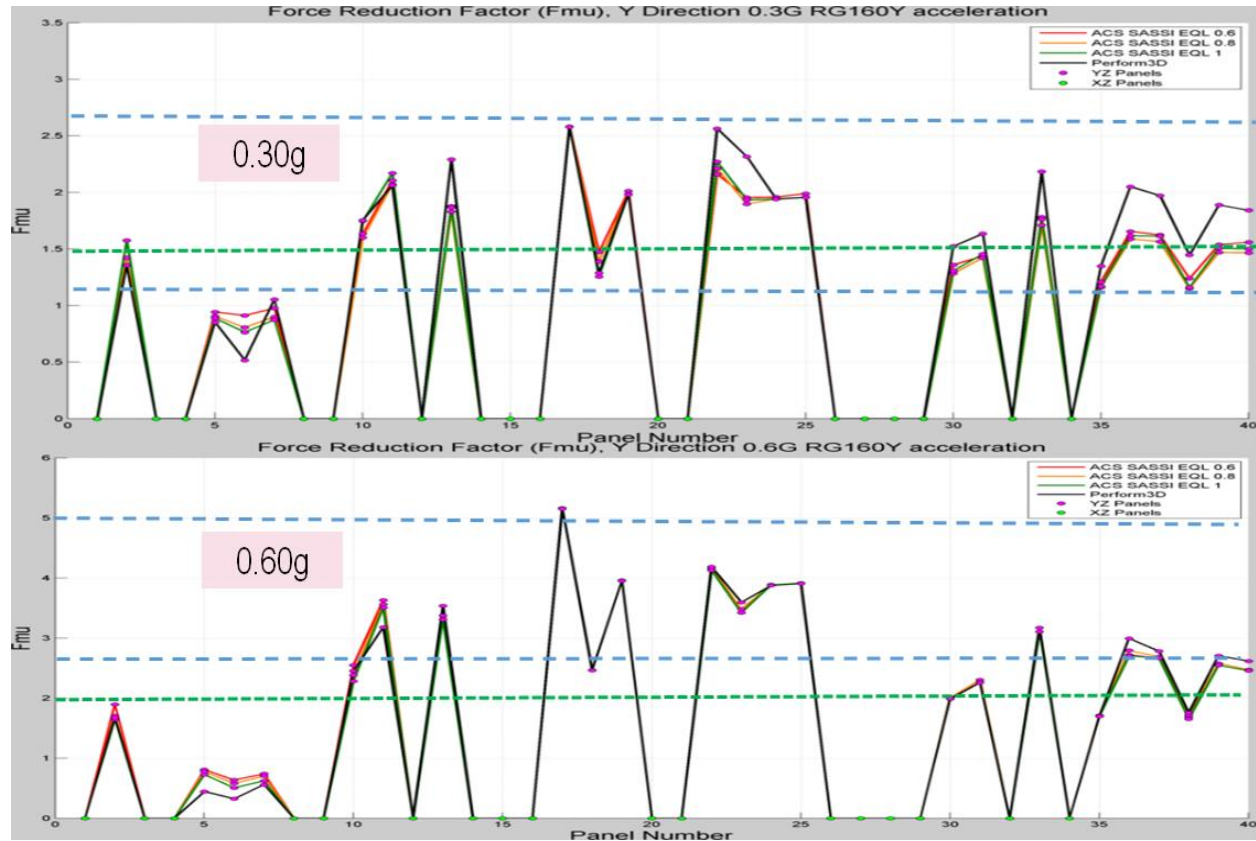


Figure 12 Shear Force Inelastic Absorption Factors for 0.30g and 0.60g Y-Direction Seismic Inputs Using ACS SASSI Hybrid Approach (color) and PERFORM3D Nonlinear Time Integration Approach (black)

Figure 12 also compares the computed inelastic absorption factors with the values provided by ASCE 43-05 standard (horizontal green dotted line) for the low-rise shearwall buildings for the limit state C (reduced yielding) for 0.30g input and limit state A (ultimate, close to collapse) for 0.60g input, respectively. On the same plots, we also included the results published by Ibarra and Chowdhury (horizontal blue dotted line) for the median and 5% non-exceedance probability values of the inelastic absorption reduction factors based on a Southwest Research Institute (SwRI) study for stiff concrete structures (Ibarra and Chowdhury, 2006).

An additional comparison between the ACS SASSI iterative approach and PERFORM3D time integration approach was done in terms of the computed in-structure acceleration response spectra (ARS) for 0.60g in Y-direction. Figure 13 shows the ISRS computed at lower and higher elevation locations. Again, there is a good matching of the nonlinear analysis results of the two FEA codes. It should be noted that the SRF values of 0.8 and 1.0 provide the best ARS matching with the nonlinear time domain results up to a frequency of 20 Hz. For higher frequencies than 20 Hz, computed ARS using PERFORM3D are much larger than linear elastic ARS. The PERFORM3D acceleration histories include large noise above 20 Hz.

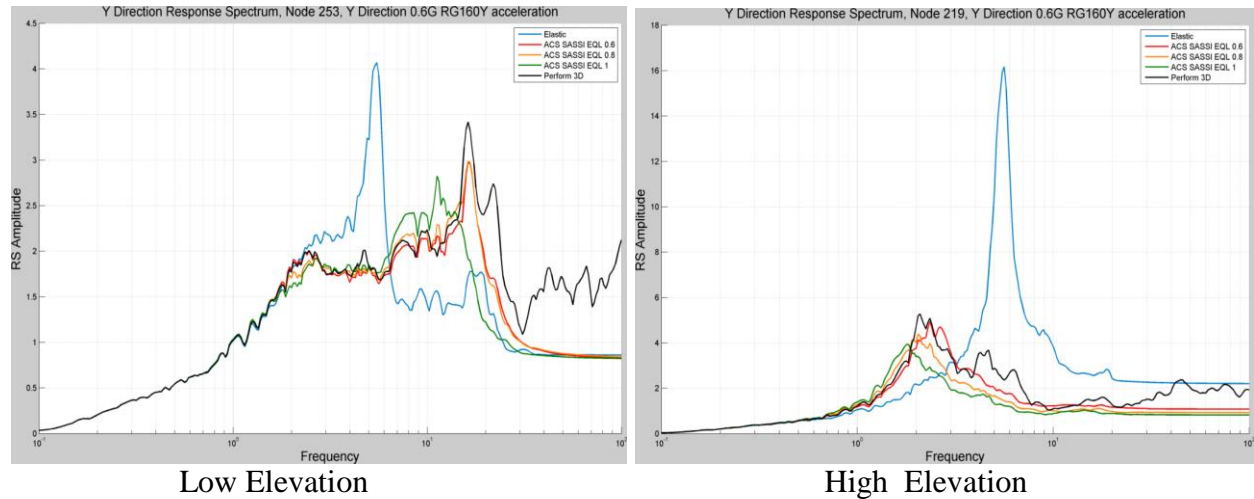


Figure 13 Elastic (blue line) vs. Inelastic ARS Computed for 0.60g Seismic Input Using ACS SASSI (3 SRF values: 0.6 red, 0.8 orange and 1.0 green) and PERFORM3D (black)

### SSI ANALYSIS CASE STUDIES FOR ROCK AND SOIL SITES

For the limited space remaining in this paper, we would like to illustrate the application of the ACS SASSI hybrid approach to the nonlinear SSI analysis of the nuclear shearwall building for a hard-rock site ( $V_s$  of 8000 fps) and a soft-soil site soil ( $V_s$  of 1000 fps). Comparative results in terms of the wall panel ductilities (computed with respect to the cracking threshold and the shear force inelastic factors for the 0.30g and 0.60g earthquake levels are provided in Table 1.

Panel	Rock Site				Soil Site			
	0.3g		0.6g		0.3g		0.6g	
	$\mu^*$	$F\mu$	$\mu^*$	$F\mu$	$\mu^*$	$F\mu$	$\mu^*$	$F\mu$
2	1.25	1.40	3.70	1.66	1.01	0.94	2.13	1.34
3	1.27	1.31	2.24	2.07	1.27	0.95	2.16	1.50
9	1.28	1.21	2.24	1.92	1.30	0.93	2.31	1.44
10	1.97	1.63	5.58	2.35	2.40	1.07	10.80	1.50
11	6.20	2.03	15.91	3.43	6.29	1.47	16.27	2.47
13	3.14	1.81	6.91	3.27	2.85	1.60	8.18	2.75
17	12.71	2.51	61.80	5.03	10.97	1.66	65.76	3.33
18	2.66	1.38	37.62	2.43	1.89	1.01	24.83	1.50
19	7.40	1.95	50.01	3.88	6.22	1.38	41.31	2.68
22	3.22	2.17	6.61	4.07	3.00	1.36	10.46	2.52
23	4.27	1.88	9.34	3.39	2.86	1.43	7.65	2.32
24	9.85	1.92	64.26	3.84	3.71	1.24	52.54	2.40
25	9.55	1.92	56.04	3.84	5.64	1.42	50.37	2.79
30	1.92	1.27	4.90	2.02	0.97	1.02	2.84	1.31
31	2.25	1.39	5.63	2.26	2.37	1.33	8.74	2.22
33	2.73	1.69	6.02	3.09	1.61	1.41	3.52	2.19
35	1.60	1.14	4.35	1.70	0.99	1.00	3.80	1.24
36	2.94	1.57	6.72	2.67	2.28	1.35	7.14	2.09
37	2.49	1.54	5.69	2.67	1.95	1.41	4.64	2.20
38	1.82	1.13	4.93	1.67	1.67	1.28	4.77	1.83
39	2.36	1.45	5.28	2.53	0.95	0.96	2.23	1.37
40	2.44	1.45	5.61	2.45	1.11	1.13	2.68	1.65
Average	3.88	1.63	16.88	2.83	2.88	1.24	15.23	2.03
Max	12.71	2.51	64.26	5.03	10.97	1.66	65.76	3.33

Note \* : The ductility ratio are computed with respect to cracking strain

Table 1. Computed Panel Ductilities (wrt cracking) and Inelastic Factors for Rock and Soil Sites

It should be noted that the wall panel inelastic factors for the soil site were 0.65-1.10 of the inelastic factors for the hard-rock site. The average and maximum inelastic factors were for the 0.30g earthquake 1.64 and 2.51 for the hard-rock site, and 1.24 and 1.66 for the soil site. For the 0.60g earthquake, the same quantities were 2.83 and 5.03 for the hard-rock site, and 2.03 and 3.33 for the soil site, respectively. The maximum inelastic factors shown in Table 1 were compared with those computed at SwRI (Ibarra and Chowdhury, 2006) for the concrete limit states C (1.5 times yielding deformation) and A (8 times yielding deformation) computed for stiff concrete structures, such as nuclear structures, with no SSI effects included. The median inelastic absorption factor values computed by Ibarra and Chowdhury were about 2.60 for limit C and 5.00 for limit A. These values compare extremely well with the inelastic factors computed using ACS SASSI for the hard-rock site in the most damaged walls that were 2.51 for limit C (for 0.30g input) and 5.03 for limit A (for 0.60g input). The differences were less than 5%.

The nonlinear SSI analysis results show that the coupling between the nonlinear structural behaviour and the SSI foundation motion. This is an important modelling aspect. The inelastic structural deformations could change severely the amplitude and frequency content of the SSI foundation rocking motion. The influence is larger for soil sites. A comparison of the SSI structural motion animations for the linear elastic structure (uncracked) and the nonlinear concrete structure is shown at [http://www.ghiocel-tech.com/enggTools/ACS\\_SASSI\\_Elastic\\_vs\\_Nonlinear\\_Response\\_For\\_Soil\\_Foundation\\_0.6g\\_Acc.avi](http://www.ghiocel-tech.com/enggTools/ACS_SASSI_Elastic_vs_Nonlinear_Response_For_Soil_Foundation_0.6g_Acc.avi). The structural animations are obtained for the 0.60g earthquake and the soil site. The structural animations indicate clearly that the assumption that *the SSI foundation motion is not influenced by the structural nonlinear behaviour*, as some researchers wrote in their recent papers, is completely wrong.

## CONCLUDING REMARKS

The presented results validate the proposed nonlinear SSI hybrid approach against the “true” nonlinear time integration approach. The nonlinear SSI hybrid approach results were also compared favourably with the results obtained by the SwRI research studies on the nonlinear behaviour of stiff concrete structures, such as nuclear structures. The nonlinear SSI hybrid approach based on an iterative linearized FEA solution in complex frequency appears to be tens to hundreds of times faster than the “true” nonlinear SSI analysis based on the time-integration approach for identical computer platforms. In addition, the hybrid approach is much more robust than the time-domain nonlinear approaches using the direct integration that are often overly noisy and overly sensitive to small input parameter variations.

## REFERENCES

- Cheng, Y.F. and Mertz, G. (1989). “Inelastic Seismic Response of Reinforced Concrete Low-Rise Shear Walls of Building Structures”, University of Missouri-Rolla, Dept. of Civil Engineering, CE 89-30
- Ghiocel Predictive Technologies, Inc. (2015). “ACS SASSI - An Advanced Computational Software for 3D Dynamic Analyses Including SSI Effects”, ACS SASSI Version 3.0 Manuals, March 31, [http://www.ghiocel-tech.com/publications/ACS%20SASSI\\_V300\\_Brief\\_Description\\_Dec\\_31\\_2014.pdf](http://www.ghiocel-tech.com/publications/ACS%20SASSI_V300_Brief_Description_Dec_31_2014.pdf)
- Gulec and Whittaker, A. and B. Stojadinovic. (2009). “Peak shear strength of squat reinforced concrete walls with boundary barbell or flanges,” *ACI Structural Journal*, Vol. 106, No. 3, pp.368-377.
- Kausel, E. and Assimaki, D. (2002). “Seismic Simulation of Inelastic Soils Via Frequency-Dependent Moduli and Damping”, *ASCE Journal of Engineering Mechanics*, Vol. 128, No.1, January
- Ibarra, L. and Chowdhury, A. (2006). “Inelastic Absorption Energy Factors for Short Period Deteriorating SDOF Systems”, 1<sup>st</sup> ECEES, Geneva, Switzerland, September 3-8, Paper 429